Quality assessment of ICESat-2 ATL03 denoising data based on spatial distribution and photon weight

Yuan Sun [1,2,3], Huan Xie [1,*], Xiaohua Tong [1], Qi Xu [1], Binbin Li [1], Changda Liu [1], Min Ji [1], and Hao Tang [2,3]

[1] College of Surveying and Geo-Informatics, Shanghai Key Laboratory for Planetary Mapping and Remote Sensing for Deep Space Exploration, Tongji University, Shanghai 200092, China – sunyuan@tongji.edu.cn, huanxie@tongji.edu.cn
[2] Department of Geography, National University of Singapore, Singapore 117570, Singapore
[3] Centre for Nature-based Climate Solutions, National University of Singapore, Singapore 117546, Singapore

Keywords: ICESat-2, Denoising, Photon Weight, Quality Assessment.

Abstract

The Ice, Cloud, and land Elevation satellite-2 (ICESat-2) adopts an advanced single photon detection system, which is susceptible to the influence of solar background noise. There are currently multiple methods for denoising ICESat-2 photon data, but due to the availability and limitations of reference data, it is difficult to evaluate the denoising results of large-scale photon data. Therefore, in this paper, we propose a quality evaluation method that does not rely on auxiliary data. By considering the spatial distribution and photon weight, it was determined whether the signal and noise photons were extracted correctly, and the precision (P), recall (R), and F-measure (F) of the denoising results were evaluated. The results showed that for the strong beam and weak beam data obtained during the day and night, the average difference between the evaluation results of this method and the true label were 0.0177, 0.0794 and 0.0018, 0.0042, respectively. In general, the quality evaluation results of this study are very close to those of the real labels, indicating that the method in this paper can effectively evaluate the quality of the denoising results.

1. Introduction

In 2018, with the successful launch of the Ice, Cloud, and land Elevation Satellite-2 (ICESat-2), the gap in Earth observation data in the field of spaceborne laser altimetry over the past decade is filled (Markus et al. , 2017). Compared with the 70 m footprint of Ice, Cloud, and land Elevation Satellite (ICESat), the footprint of the Advanced Topographic Altimeter System (ATLAS) equipped on ICESat-2 is only 12 m, with a sampling interval of 0.7 m along the track, which can collect data with higher resolution and has unique advantages in obtaining large-scale ice sheet elevation changes, sea ice density estimation, and forest canopy height inversion (Magruder et al. , 2020). ICESat-2 uses a single-photon sensitive detection mechanism and a 532 nm green laser to measure the two-way flight time of a single photon, and then calculate the latitude, longitude and surface height of each received photon (Neumann et al. , 2019). However, the laser altimeter is very sensitive to sunlight, so there are not only signal photons in the downlinked data, but also a lot of background noise caused by sunlight. At present, although the ICESat-2 team has identified and labelled the signal and noise photons, the accuracy of the identification has not yet been given.

Currently, multiple studies have evaluated the quality of ICESat-2 products. The first category is to assess the positioning accuracy of ICESat-2: Schenk et al. (2022) used high-precision digital elevation model (DEM) data to evaluate the horizontal accuracy of ICESat-2 in the McMurdo Dry Valley region of Antarctica. Luthcke et al. (2021) also used high-precision DEM data to validate pointing and geolocation errors of ICESat-2. The second category is to evaluate the surface height of ICESat-2: Zhao et al. (2022) used airborne LiDAR data to verify the surface height of ATL03 and ATL08 products. Kwok et al. (2019) used Airborne Topographic Mapper (ATM) lidar to verify the surface height and sea ice freeboard of ATL07 and ATL10 products. Brunt et al. (2019) used global navigation satellite system (GNSS) data to verify the height of the Antarctic ice sheet. Li et al. (2021) used multiple sensor observation methods including GNSS, unmanned aerial vehicle (UAV), and corner cube retroreflector (CCR) to verify the surface elevation of sea ice. The third category is to evaluate the classification results of ICESat-2: Petty et al. (2021) used Sentinel-2 Imagery to verify the classification algorithm of ICESat-2. These quality evaluation methods mostly utilize more accurate external auxiliary data for evaluation. However, in the absence of external data, how to evaluate the quality based on the data itself is still in urgent need of research, so that a large-scale quality evaluation can be performed on all the acquired data.

This study evaluates the quality of denoising results based on the spatial distribution and weight of photons. The main innovations are as follows: the denoising results can be evaluated without external data; the weight of photons is added to distinguish misclassified signals from noise.

2. Methods

2.1 ATL03 Data

The ATL03 data product is a very basic product in the ICESat-2 product system, which includes the time, longitude, latitude, and elevation values of each photon. It is also the input data for producing higher-level products such as segmented and grid data of land ice, land and so on. ATL03 contains the ‘signal_conf_ph’ parameter, which is an array of N*5 columns with a value range of -2-4, representing possible transmitter echo path photon, not considered photon, noise photon, buffer photon, low confidence photon, medium confidence photon, and high confidence photon. In general, photons with a value greater than 1 represent signal photons.

The data used in this paper are the sixth edition of data released by National Snow and Ice Data Cente (NSIDC), and the download website is https://nsidc.org/data/data-access-tool/ATL03/versions/6. The sixth edition of data uses the data of the 20m segment to calculate the KNN mean inverse vertical distance between the photon and the K nearest photon, and obtains the weight of each photon. The value ranges from 0 to 255. The larger the value, the greater the probability that the

photon belongs to the signal. It is the key parameter used in this study.

The experimental area is an urban area located in Zhengzhou City, Henan Province, China. Two sets of experimental data were collected during the day and at night, respectively, each containing six beams, so that the impact of day and night, strong beams and weak beams on the algorithm can be compared. The distribution and data description of the experimental data are shown in Figure 1 and Table 1 below, where the black line represents strong beams and the grey line represents weak beams, with a total of 24 beams.

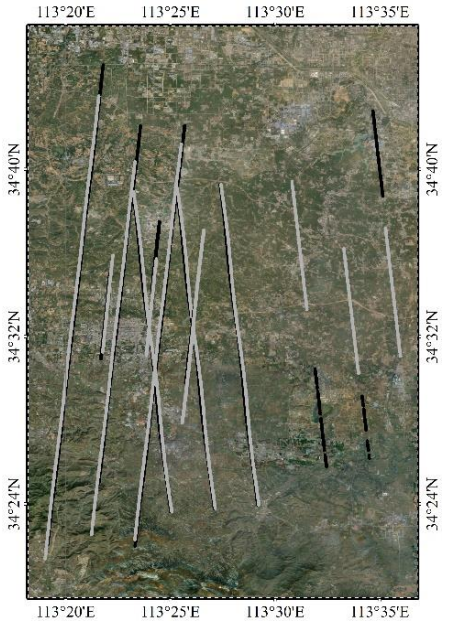

Figure 1. Locations of the study sites with different beam types [background image source: Esri, Maxar, GeoEye, Earthstar Geographics, CNES/Airbus DS, USDA, USGS, AeroGRID, IGH, and the GIS User Commmity].

Table 1. Overview of the ICESat-2 datasets.

ID	Dataname	Time	Track ID
D1	ATL03_20200422172616_04150706_006_02.h5	Night	GT1L~GT3R
D2	ATL03_20190930150630_00570502_006_02.h5	Night	GT1L~GT3R
D3	ATL03_20190725062644_04150406_006_02.h5	Day	GT1L~GT3R
D4	ATL03_20190101040709_00570202_006_02.h5	Day	GT1L~GT3R

2.2 Calculation of Precision

After extracting the signal photons, they are divided into upper and lower parts, with a processing unit size of one segment (nominally 20 m along track). For each part of the signal photons, sort them according to elevation, and record the height difference between the photon and adjacent photons as $diff_{upper}$ and $diff_{low}$. The larger the height difference, the higher the probability that the signal photon belongs to noise photons.

For the upper and lower parts of the signal photons, perform the following calculations for each part: find the index of photons i_1 with a height difference value outside the range of $\mu + 2\sigma$, and the index of photons i_2 with the highest height difference value, and the number of photons i_3 with a weight value lower than the given threshold (default value of 50) for each part. Determine whether the weight range of the photons within the above index range is below the threshold. If it is below the threshold, it is considered noise, otherwise it will still be retained as signal photons. For a specific schematic diagram, please refer to Figure 2 below. The calculated i_1, i_2 and i_3 in the upper and lower parts are all 1, corresponding to two blue photons, and both photons have passed the weight threshold test, indicating that these two photons are misclassified signal photons. Then, according to this process, the signal photons in each segment are judged, and the number of photons that are truly signal photons among the signal photons identified by the ATL03 algorithm is calculated, so as to calculate precision (P).

$$P = \frac{QS_S}{QS_S + AT_S} \tag{1}$$

where QS_S = the number of signal photons in the quality evaluation result

AT_S = the number of photons judged as signals by ATL03 and judged as noise photons by this method.

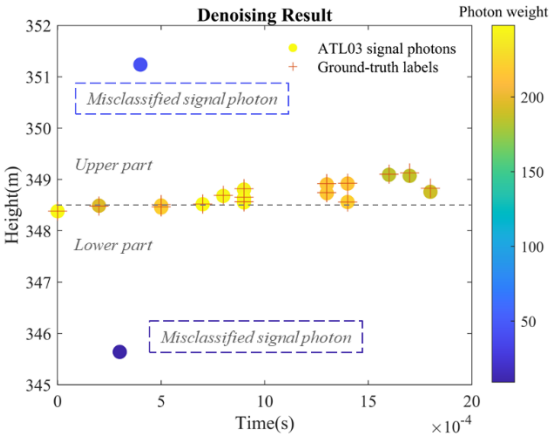

Figure 2. Schematic diagram of calculation of precision.

2.3 Calculation of Recall

Find the noise photons near the signal photons, divide them into two parts based on the average elevation of the signal photons, and perform the following calculation for each part of the upper and lower parts: first, determine the search range for noise photons. The terrain undulation value is obtained based on the difference between the maximum and minimum elevations of the signal photons in this data segment. If the number of noise photons with weights greater than 100 in this data segment is greater than 10% of the number of noise photons, the search range is set to 10% of the undulation value. Otherwise, the search range is set to 15 m. Figure 3 (a) shows all the photon data within the original photon profile, while Figure 3 (b) shows noise photons within the search range. Since the noise photon data outside the search range is far from the terrain, the photons outside the search range are not considered in the calculation process of recall (R). For noise photons within the search range above and below the signal location, continuously add it to the existing signal photons, and determine the change in the elevation standard deviation of the signal photons before and after addition. For each segment of data, a histogram is established by combining the signal photons of the two preceding and following segments. If the noise photon is within the range of the bin where the signal peak is located, it is considered a signal photon; Otherwise, determine the weight value. If the weight is greater

than the threshold, it is considered a signal, otherwise it is still noise. Based on the re-judgment of noise photons, the R value is calculated.

$$R = \frac{QS_S}{QS_S + AT_N} \quad (2)$$

where QS_S = the number of signal photons in the quality evaluation result

AT_N = the number of photons judged as noises by ATL03 and judged as signal photons by this method.

The F-measure (F) value is calculated based on the P-value and R-value.

$$F = \frac{2P \cdot R}{P + R} \quad (3)$$

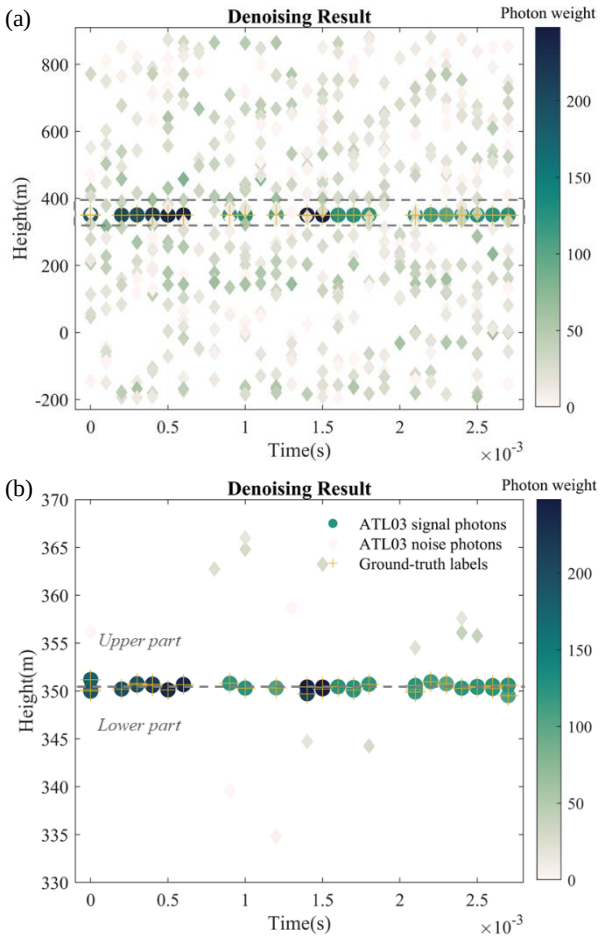

Figure 3. Schematic diagram of calculation of recall. (a) All the photon data distribution in the original photon profile. (b) The noise photon distribution in the search range.

2.4 Performance Assessment

For the selected experimental data, we performed label correction on the ATL03 denoising results, and then compared the ATL03 denoising results with the labels to obtain the evaluation index P_l, R_l, and F_l value. The P, R, and F value obtained in the previous two steps is compared with this P_l, R_l, and F_l value and the differences are calculated, so that the accuracy of the quality evaluation results can be obtained.

$$\Delta P = P - P_l \quad (4)$$

$$\Delta R = R - R_l \quad (5)$$

$$\Delta F = F - F_l \quad (6)$$

3. Results

Figure 4 shows the strong beam data obtained during the daytime on July 25, 2019 (data name: ATL03_20190725062644_04150406_006_02.h5). Figure 4 (a) shows the denoising results obtained by the ATL03 algorithm, Figure 4 (b) shows the denoising results obtained after quality evaluation correction, and Figure 4 (c) shows the denoising labels obtained by visual interpretation. In general, the original denoising results are relatively rough. This is because ATL03 algorithm adds a buffer when identifying signals in order to identify more signal photons. Therefore, some abnormal points are clearly seen, especially the signal photons within the time range [49271594, 49271594.5]. After quality evaluation, the extraction results of this section of signal photons have improved, and the overall range of signal photons has also been reduced, which is reflected in the reduction of the width of the blue curve composed of signal photons. The ground trends of the Figure 4 (b) and Figure 4 (c) are relatively consistent, and the elevation ranges of signal photons are very similar, indicating that the signal photons after quality evaluation are relatively consistent with the real labels.

According to the Figure 5, this method can correct misclassified signal photons, such as photons within the time range of [49271594.14, 49271594.16], and blue non-topographic signal photons that are corrected to noise photons after quality evaluation. The terrain photons that were originally classified as noise photons can also be re-identified as signal photons, such as photons within the time range of [49271594.18, 49271594.2], and the originally grey terrain photons can be re-identified as signals and labelled as blue.

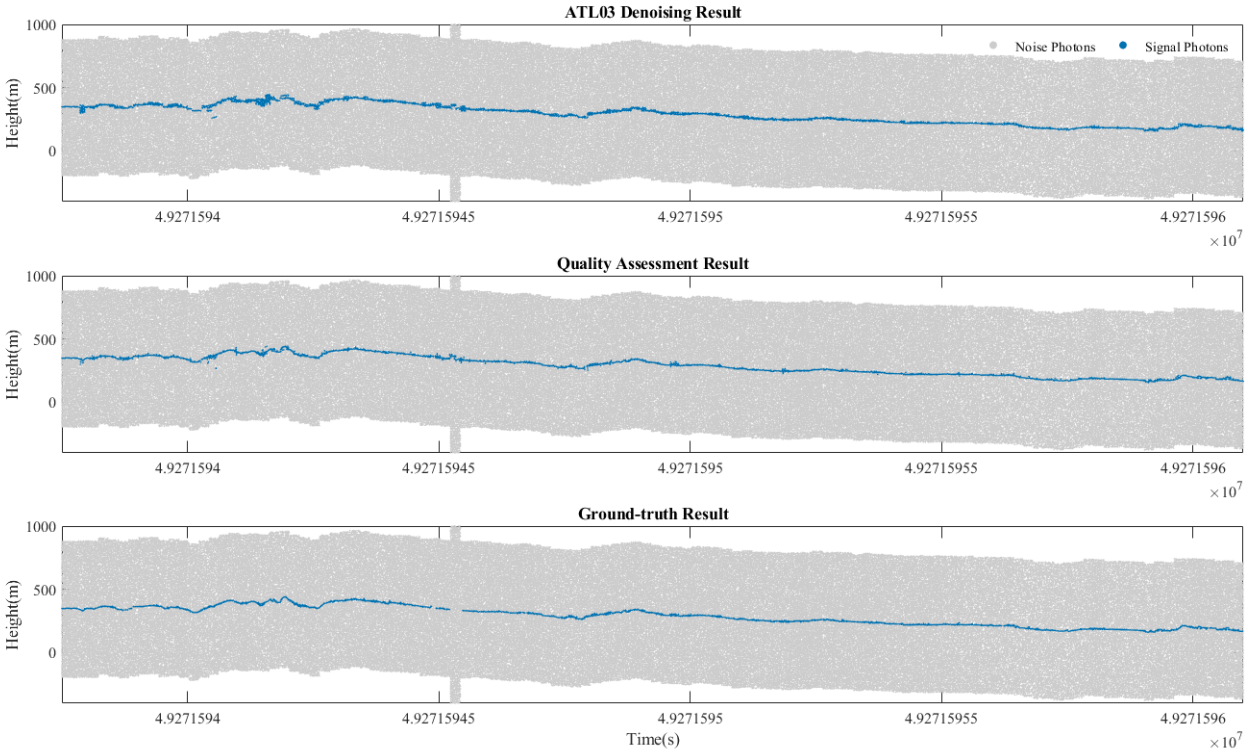

Figure 4. Comparison of denoising results. (a) Denoising result obtained by ATL03 algorithm. (b) Denoising result obtained after quality evaluation correction. (c) Denoising result labels obtained by visual interpretation.

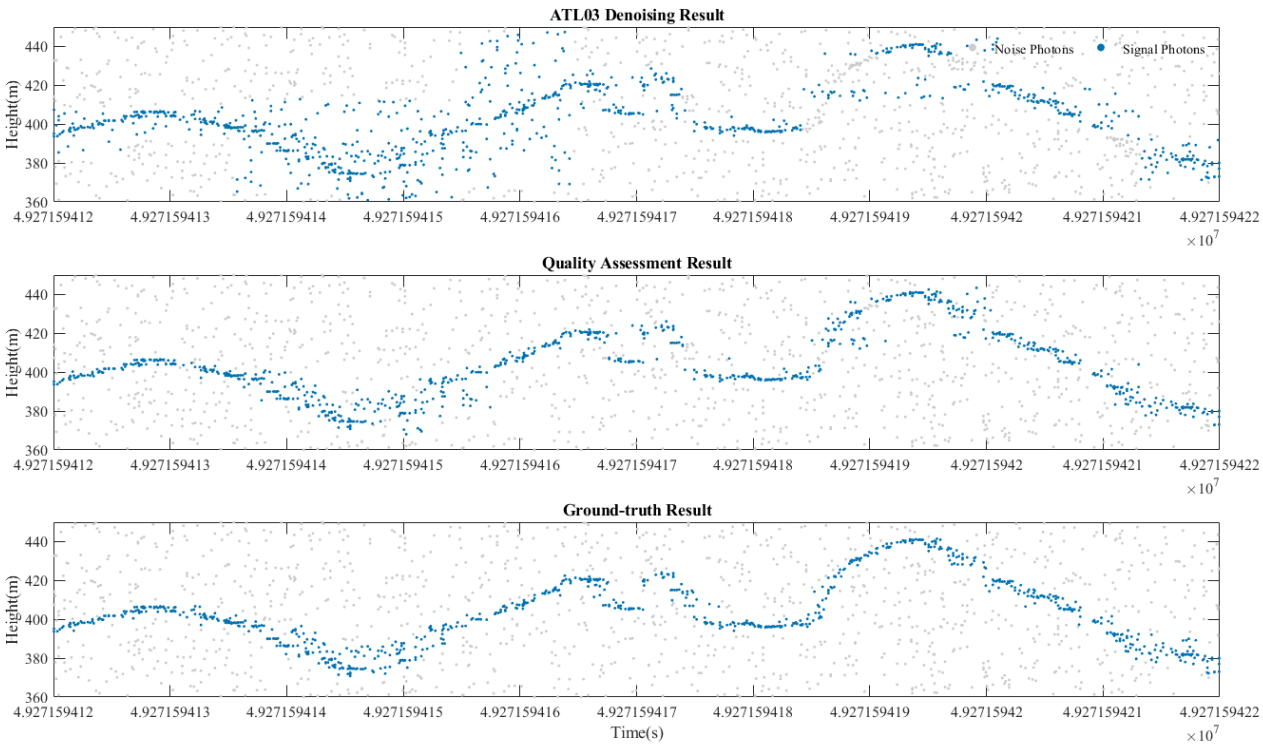

Figure 5. Enlarged display of Figure 4 within the time range of [49271594.12 49271594.22].

This paper selected a total of four data sets acquired during the day and at night, each containing six beams. First, according to the visually interpreted labels, the denoising results of ATL03 were compared with the label results to obtain the real P_l, R_l, and F_l value. Then, the denoising results of ATL03 were compared with the quality evaluation results of this study to obtain the calculated P, R, and F value. Finally, the real and calculated P, R, and F values were subtracted to obtain ΔP, ΔR, and ΔF. Figure 6

below shows the data acquired during the day, where Di_j represents the j-th pair of beams of the i-th data. Light green and dark green are the evaluation indicators for comparing the quality evaluation results of weak beams and strong beams with the true labels, respectively. Light green has a larger fan-shaped area, indicating a significant difference from the result of the true label. Since the weak beam has low energy and a small number of signal photons, the quality evaluation of the weak beam is more difficult. The small area occupied by dark green indicates that the difference between the results and the real label is small. Due to the high energy of the strong beam and the large number of signal photons, this article provides more accurate recognition of misclassified photons.

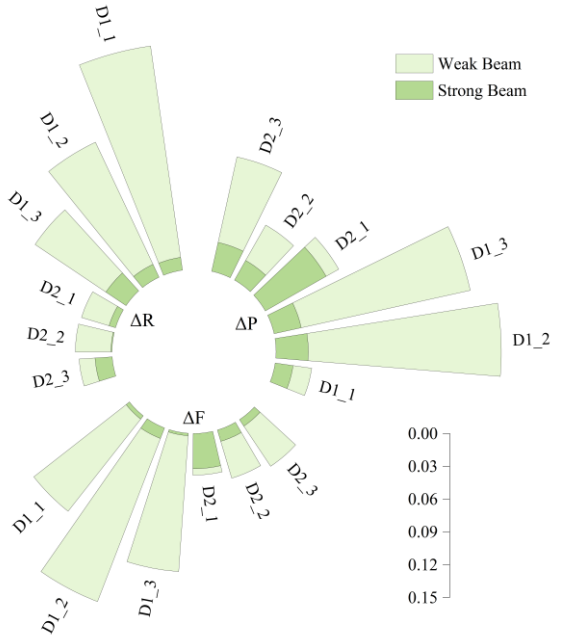

Figure 6. Comparison of the quality evaluation results between this method and the real label during the daytime.

Figure 7 below shows the data acquired at night. The light blue and dark blue are the evaluation indicators of the quality evaluation results of weak beams and strong beams compared with the true labels. The light blue sector area is larger, indicating that the results are significantly different from the true labels, which is consistent with the conclusion of the data acquired during the day. However, compared with the data acquired during the day, the deviation of the weak beam is 6 to 8 times that of the strong beam, and the deviation of the weak beam acquired at night is only 2 to 3 times that of the strong beam. Therefore, the quality evaluation accuracy of the night data is higher. The smaller area occupied by the dark blue indicates that the difference with the true label result is smaller, which is consistent with the conclusion of the data acquired during the day. There are fewer noise photons at night, so the difficulty of identifying signal photons is small, so the quality evaluation results of this article are more accurate.

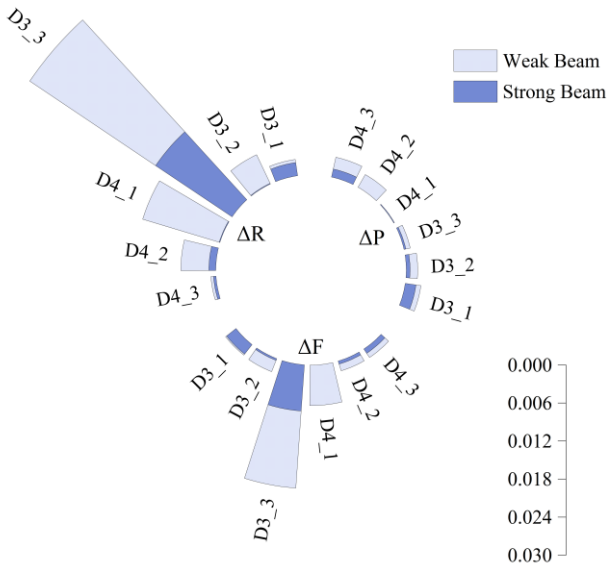

Figure 7. Comparison of the quality evaluation results between this method and the real label at night.

In general, the mean difference between the quality evaluation results and the label results obtained by strong beams and weak beams during the day is 0.0177 and 0.0794 respectively, and the mean difference between the quality evaluation results and the label results obtained by strong beams and weak beams at night is 0.0018 and 0.0042 respectively. The difference of the data obtained during the day is generally larger than that at night, indicating that the quality evaluation results at night are better. At the same time, the difference of the strong beam is smaller than that of the weak beam, which also shows that the quality evaluation results of the strong beam are better.

4. Conclusions

This paper proposes a quality evaluation method for ATL03 data that does not require auxiliary data. It can evaluate the denoising results of ATL03 and provide the P, R, and F value. First, the height difference and weight values of different photons and their neighboring photons are calculated to obtain the P, R, and F of the signal photon. Afterwards, the noise photons are judged one by one, and the recall is calculated. Based on P and R values, F is calculated. Finally, the P_l, R_l, and F_l of the signal photon obtained by ATL03 and the real label is calculated, and compared with the P, R, and F of this method. The results show that the calculated P, R, and F are very close to the real P, R, and F, with a deviation of less than 0.0794 during the day and less than 0.0042 at night. The quality evaluation results at night are better than those during the day, and the quality evaluation results of strong beams are better than those of weak beams, indicating that this method can effectively evaluate ATL03 data obtained at different times.

Funding

This research was supported by the National Natural Science Foundation of China [grant number 42325106 and 42221002], the Shanghai Academic Research Leader Program [grant number 23XD1404100], the Fundamental Research Funds for the Central Universities of China and the China Scholarship Council [grant number 202406260317].

References

Brunt, K.M., Neumann, T.A., Smith, B.E. Assessment of ICESat-2 Ice Sheet Surface Heights, Based on Comparisons Over the Interior of the Antarctic Ice Sheet. Geophys. Res. Lett. 46, 13072-8, 2019.

Kwok, R., Kacimi, S., Markus, T., et al. ICESat-2 Surface Height and Sea Ice Freeboard Assessed With ATM Lidar Acquisitions From Operation IceBridge. Geophys. Res. Lett. 46, 2019.

Li, R., Li, H., Hao, T., et al. Assessment of ICESat-2 ice surface elevations over the Chinese Antarctic Research Expedition (CHINARE) route, East Antarctica, based on coordinated multi-sensor observations. Cryosphere 15, 3083-99, 2021.

Luthcke, S.B., Thomas, T.C., Pennington, T.A., et al. ICESat-2 Pointing Calibration and Geolocation Performance. Earth Space Sci. 8, 2021.

Magruder, L.A., Brunt, K.M., Alonzo, M. Early ICESat-2 on-orbit Geolocation Validation Using Ground-Based Corner Cube Retro-Reflectors. Remote Sens-Basel 12, 3653, 2020.

Markus, T., Neumann, T., Martino, A., et al. The Ice, Cloud, and land Elevation Satellite-2 (ICESat-2): Science requirements, concept, and implementation. Remote Sens. Environ. 190, 260-73, 2017.

Neumann, T.A., Martino, A.J., Markus, T., et al. The Ice, Cloud, and Land Elevation Satellite – 2 mission: A global geolocated photon product derived from the Advanced Topographic Laser Altimeter System. Remote Sens. Environ. 233, 111325, 2019.

Petty, A.A., Bagnardi, M., Kurtz, N.T., et al. Assessment of ICESat-2 Sea Ice Surface Classification with Sentinel-2 Imagery: Implications for Freeboard and New Estimates of Lead and Floe Geometry. Earth Space Sci. 8, 2021.

Schenk, T., Csatho, B., Neumann, T. Assessment of ICESat-2 ' s Horizontal Accuracy Using Precisely Surveyed Terrains in McMurdo Dry Valleys, Antarctica. IEEE Trans. Geosci. Remote Sens. 60, 2022.

Zhao, Y., Wu, B., Shu, S., Yang, L., Wu, J., Yu, B. Evaluation of ICESat-2 ATL03/08 Surface Heights in Urban Environments Using Airborne LiDAR Point Cloud Data. IEEE Geoscience and Remote Sensing Letters 19, 2022.